AAS 09-435

LEVERAGING FLYBYS OF LOW MASS MOONS TO ENABLE AN ENCELADUS ORBITER

Nathan J. Strange*, Stefano Campagnola†, and Ryan P. Russell‡

As a result of discoveries made by the Cassini spacecraft, Saturn's moon Enceladus has emerged as a high science-value target for a future orbiter mission. However, past studies of an Enceladus orbiter mission found that entering Enceladus orbit either requires a prohibitively large orbit insertion ΔV ($>$ 3.5 km/s) or a prohibitively long flight time. In order to reach Enceladus with a reasonable flight time and ΔV budget, a new tour design method is presented that uses gravity-assists of low-mass moons combined with v-infinity leveraging maneuvers. This new method can achieve Enceladus orbit with a combined leveraging and insertion ΔV of $\sim$1 km/s and a 2.5 year Saturn tour.

INTRODUCTION

In 2005, the Cassini-Huygens mission discovered water geysers erupting from the south pole of Saturn's moon Enceladus. Subsequent investigations by Cassini have provided evidence that Enceladus may have a sub-surface reservoir of liquid water with astrobiological potential. These exciting discoveries have elevated Enceladus to a high priority target for future missions by both NASA and ESA.[1,2] However, an Enceladus orbiter is a difficult mission that will require the development of new astrodynamics techniques beyond those used for the Cassini-Huygens mission.

Among many challenges in designing a trajectory for an Enceladus mission, the two most prominent arise because Enceladus is a low mass moon (its GM is only $7\ km^2/s^2$), deep within Saturn's gravity well (its orbit is at 4 Saturn radii). Designing a ΔV-efficient rendezvous with Enceladus is the first challenge, while the second involves finding a stable orbit which can achieve the desired science measurements. A paper by Russell and Lara[3] has recently addressed the second problem, and the current paper will address the first.

The Cassini orbiter is able to achieve a wide variety of orbit geometries using Titan gravity-assists (that can provide Cassini more than 800 m/s of ΔV per flyby). However, the remainder of Saturn's moons are much less effective for gravity-assists than Titan. The next largest moon, Rhea, has only 2% of Titan's mass and Enceladus has only 0.8% of Titan's mass.

In the patched-conic model, the smallest achievable v_∞ for transfers between moons is that of the Hohmann transfer. Table 1 lists the average Hohmann transfer v_∞s for those of Saturn's major moons that are in near-circular, near-equatorial orbits. From this table we see that, if we only use Titan flybys, the lowest energy transfer to Enceladus is the Hohmann transfer with a v_∞ of 3.7 km/s, which corresponds to a ΔV of 3.6 km/s to enter a 100 km circular orbit. However, if we could reach

*Senior Engineer, Jet Propulsion Laboratory / California Institute of Technology, 4800 Oak Grove Drive, Pasadena, CA, 91109

†Ph.D. Candidate, University of Southern California, 854 Downey Way, Los Angeles, CA, 90089

‡Associate Professor, Georgia Institute of Technology, 270 Ferst Drive, Atlanta, GA, 30332

Tethys and then use a Hohmann transfer from Tethys to Enceladus the required v_∞ would drop to 0.62 km/s and the ΔV to enter a 100 km circular orbit would drop to only 0.53 km/s.

Table 1. Hohmann Transfer V-Infinities [km/s]

v_∞ *wrt.*	*Hohmann transfer connects to:*					
moon:	Mimas	Enceladus	Tethys	Dione	Rhea	Titan
Mimas	0.00	0.86	1.54	2.26	3.10	4.55
Enceladus	0.81	0.00	0.65	1.36	2.20	3.71
Tethys	1.37	0.62	0.00	0.68	1.51	3.06
Dione	1.89	1.21	0.64	0.00	0.80	2.37
Rhea	2.36	1.79	1.30	0.73	0.00	1.54
Titan	2.71	2.39	2.10	1.74	1.25	0.00

Table 1 suggest that an economical orbit insertion at Enceladus may be achieved by stringing together a set of Hohmann (or near-Hohmann) transfers from Titan, to Rhea, to Dione, to Tethys, and then to Enceladus. However, such a string of Hohmann transfers requires a 180° rotation of the v_∞ vector at each moon as the spacecraft switches from an orbit with flybys of a moon near periapsis of the Saturn-centered orbit to flybys near apoapsis. With the low mass of these moons, a conventional tour as described could take over 7 years.[1]

For example, if we start from a Titan-Rhea Hohmann, the Rhea flyby v_∞ would be 1.54 km/s. At this v_∞, a 50 km flyby gives 8.5° of bending and it would take at least 22 flybys to rotate the v_∞ vector by 180°. However, in practice it will take more than 22 Rhea flybys as each flyby must place the spacecraft in an orbit that returns to Rhea and such transfers are not conveniently spaced at 8.5° intervals. That is, unless maneuvers can be used somehow to make up for the lack of bending provided by the Rhea flybys.

This strategy of using maneuvers to make up for the limited bending from these small moons was done in an ad hoc manner for a 2007 JPL Rapid Mission Architecture (RMA) study of possible Enceladus missions.[4] For this RMA study an early version of the methods presented in this paper was used to construct a (fully-integrated) trajectory that reached Enceladus orbit with 3.5 km/s of ΔV and a 3.5 year flight time from Saturn Orbit Insertion (SOI). The further development of these techniques in this paper has enabled a substantially improved design with 2.3 km/s of ΔV and a 2.5 year flight time from SOI. Furthermore, this new design eliminates the 25 km flybys of Rhea and Tethys required by the RMA study trajectory.

V-Infinity Leveraging Transfers

For spacecraft trajectories using gravity assists, a spacecraft's v_∞ (i.e. hyperbolic excess velocity) relative to a gravity-assist body cannot usually be changed without a gravity-assist from another body or a maneuver. *Leveraging* maneuvers[a] change a spacecraft's v_∞ when a gravity assist from another body isn't available to do it for free. A small leveraging maneuver can translate into a change in v_∞ ten or more times larger than the maneuver. As the bending provided by a flyby is a

[a]V-infinity "leveraging" is a term first coined by Longuski and first documented by Williams,[5] Longuski's student. It is intended to evoke the gravity-assist tour design terminology of "pumping" (changing orbit period) and "cranking" (changing orbit inclination).[6]

function of the flyby v_∞, leveraging maneuvers provide an economical way to influence the efficacy of a flyby.

V-infinity leveraging decreases v_∞ by making the orbit around the central body more circular, and increases v_∞ by making that orbit more eccentric. For *exterior leveraging* a maneuver is done near apoapsis that raises periapsis to lower v_∞ , or lowers periapsis to increase v_∞ . *Interior leveraging* uses a maneuver at periapsis to change v_∞ by changing the orbit's apoapsis.

Past work[5,7–13] in V-Infinity Leveraging Transfers (VILTs) has largely focused on *tangent leveraging*, i.e. leveraging where the v_∞ vector is tangent to the gravity-assist body's velocity vector at one end of the transfer. For example, an exterior VILT that reduces v_∞ would use a maneuver at apoapsis to raise periapsis to the gravity-assist body's orbital distance. Therefore, a tangent VILT would achieve the maximum reduction in v_∞ for a given apoapsis radius. For large gravity-assist bodies such as planets, the Galilean satellites, Titan, and Triton, tangent VILTs are very efficient at changing v_∞ for a given transfer time.

In this application where we want to rotate the v_∞ vector by 180°, such tangent leveraging may undo rotation provided by flybys before the VILT. For example, when going from a Titan-Rhea Hohmann (with Rhea at periapsis) to a Rhea-Dione Hohmann (with Rhea at apoapsis), we would start out with $\vec{v}_\infty$ in the direction of Rhea's velocity vector (i.e. $\vec{v}_{ga}$) and end with $\vec{v}_\infty$ in the opposite direction. Exterior tangent VILTs to reduce v_∞ will tend to move periapsis back to Rhea and undo the bending of flybys in moving $\vec{v}_\infty$ away form the direction of $\vec{v}_{ga}$. Even though lower v_∞ would allow more bending per flyby, the bending towards $\vec{v}_{ga}$ from the tangent VILT could lead to requiring even more Rhea flybys to reach the goal of rotating $\vec{v}_\infty$ opposite $\vec{v}_{ga}$. In this paper, we will look at non-tangent VILTs as a way to balance the larger bending provided by lower v_∞ against the tendency for leveraging to sometimes rotate pump angle opposite to the intended direction.

Resonance Hopping

When constructing a sequence of flybys using only one gravity-assist body, three types of transfers between flybys are available.[6,10,14] *Resonant transfers* are transfers where the flight time between flybys is an integer multiple of the gravity-assist body's period, T_{ga}. Because of this, both flybys of a resonant transfer occur at the same location in the gravity-assist body's orbit. *Non-resonant transfers* are transfers where the flight time of the transfer is not a integer multiple of T_{ga} but is such that the spacecraft is still able to re-encounter the gravity-assist body. The flybys of a non-resonant transfer occur at different locations in the gravity-assist body's orbit. *Backflip transfers* (also referred to as *pi-transfers*), are a special case of a non-resonant transfer where the two flybys occur half a rev apart in the gravity-assist body's orbit. Because of the locations of the flybys, both resonant transfers and backflip transfers may be inclined, but non-resonant transfers must be in the plane of the gravity-assist body's orbit.

Compared to non-resonant and backflip transfers, resonant transfers are simple to analyze, as their period is simply $(N/M)T_{ga}$, where N is the number of gravity-assist body revs, and M is the number of spacecraft revs. Because of this, a special kind of tour called *resonance hopping*[6,15] is often used to estimate how quickly a given gravity-assist body can change the spacecraft's orbit around a central body. For a set of resonant transfers, labeled N:M , the flight time of a resonance hopping tour is simply the sum of the N's for each resonant orbit multiplied by T_{ga}. A gravity-assist body with strong gravity can hop between resonant orbits with low values of N using only a few flybys, while a body with weaker gravity often forces the choice of high N resonances which result

in longer flight times.

Figure 1 illustrates how a resonance hopping tour may be constructed using Rhea. This figure shows resonant transfers as vertical lines on a plot of orbit resonance (i.e. T_{sc}/T_{ga}) versus flyby v_∞. As flyby v_∞ approaches 0, the spacecraft orbit cannot be much different from the gravity-assist body's orbit and certain resonances become unavailable (hence the cessation of the vertical lines for lower v_∞'s). In Fig. 1 it is important to note the gaps around certain low N resonances such as 1:1, 2:1, 1:2, and 3:2. This consequence of the spacing of rational numbers on the number line can make it difficult to resonance hop near these low N resonances.

The shaded area in Fig. 1 shows all resonances that can be either reached from a 1:1 resonance or that may reach a 1:1 resonance with a single Rhea flyby of 50 km or higher. The width of this region is determined by the bending from a flyby, which is a function of v_∞ as shown in Eqn. 1:[b]

$$\sin\left(\frac{\delta}{2}\right) = \frac{\mu_{ga}}{\mu_{ga} + r_{pfb} v_\infty^2} \tag{1}$$

and by the pump angle[6] (α) required for a given resonance. Pump angle is discussed in the next section, and it is also a function of v_∞. For flybys that do not change inclination (i_{sc}), the change in pump angle is simply the bending angle.

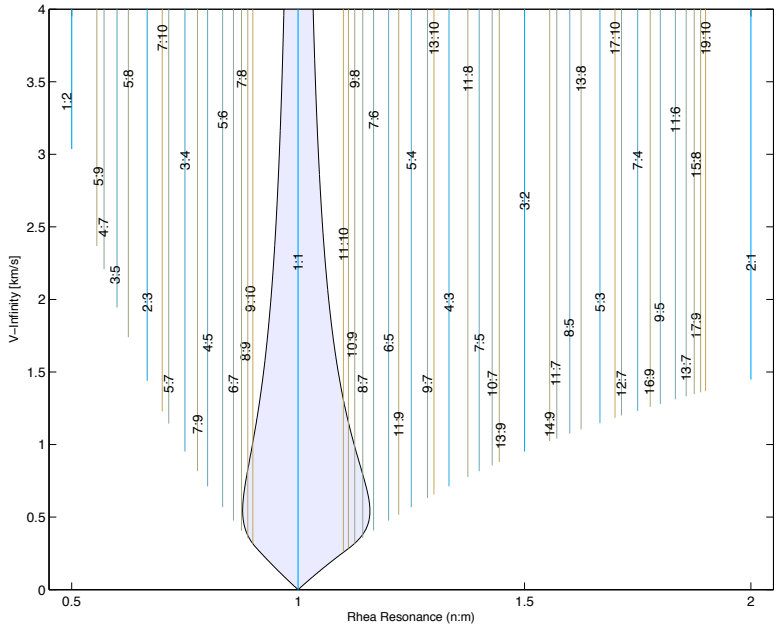

Figure 1. Resonances available to/from 1:1 Rhea resonance with 50 km flyby

From Fig. 1, we see that the resonances with the lowest N that can reach a 1:1 are 8:9 and 8:7. To hop between a 1:1 and a 8:9 or 8:7 requires a v_∞ between 0.4 km/s and 0.8 km/s. If the spacecraft v_∞ is outside of this range, a longer transfer with a higher N is required such as a 10:11 or a 12:11.

[b] All symbols used in this paper are defined in the Notation section at the end.

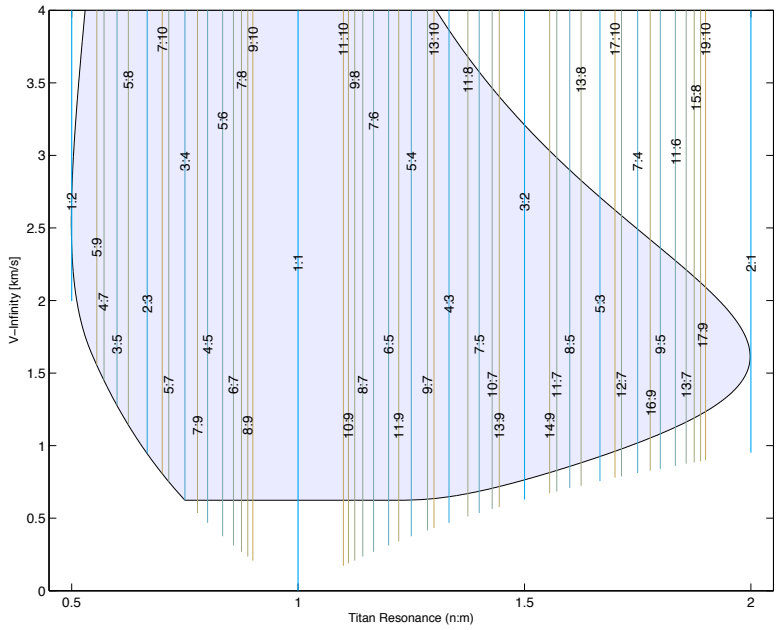

Figure 2. Resonances available to/from 3:4 Titan resonance with 850 km flyby

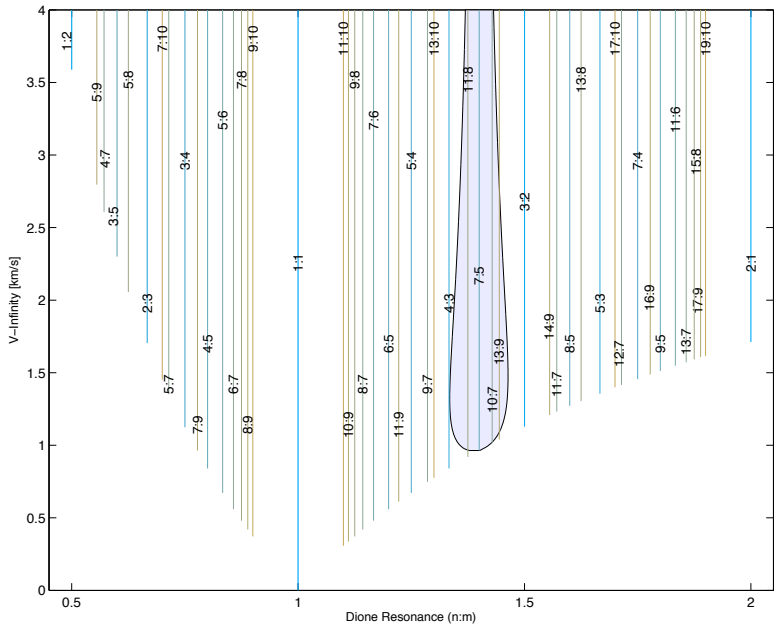

Figure 3. Resonances available to/from 7:5 Dione resonance with 50 km flyby

Figure 2 shows a similar plot for Titan where the shaded area represents orbits that can hop from or to a 3:4 resonance with a single 850 km flyby. To hop between a 2:1 and a 3:4 requires a v_∞ of $\sim$1.6 km/s, and to hop between 1:2 and 3:4 requires a v_∞ between $\sim$2.4 and $\sim$2.7 km/s. This means that a Titan resonance hoping tour from 2:1 to 3:4 to 1:2 would require changing the spacecraft v_∞. For Titan, where the shaded region covers most of the plot, it is probably better to choose a different sequence of resonances that don't require a change in v_∞. However, for smaller moons where the shaded area is much smaller changing the choice of resonances may be a larger penalty. Consider Fig. 3, which shows hopping from or to a 7:5 resonance with a 50 km flyby. For a v_∞ of $\sim$1.3 km/s a hop from 7:5 to 4:3 is possible. But without this v_∞ the hop must be to 11:8 and then 4:3, a flight time difference of 11 Dione revs (30 days). Being able to modulate the spacecraft v_∞ to make efficient resonance hops would enable savings in flight time at many such places in a tour. This is the motivation for the development of non-tangent VILTs that allow targeting of specific v_∞ values chosen for optimal resonance hoping.

ANALYSIS

For the analysis section of this paper, we will nondimensionalize the equations so that we may apply the results to any gravity-assist body. We will divide all distances by r_{enc}, the distance between the gravity-assist body and the central body at the time of the encounter. We will divide all velocity by v_c, the circular orbit velocity at r_{enc}, and time by T_c, the period of that circular orbit. With this standard, if we assume that the gravity-assist body is in a circular orbit, then $v_{ga} = 1$.

The V-Infinity Triangle

The time of a flyby yields the position and velocity of the gravity-assist body. In the patched-conic model,[16–19] the spacecraft position is assumed to be the same as the gravity-assist body at this time. And by Eqn. 2, once we know $\vec{v}_\infty$, we can get the spacecraft's velocity ($\vec{v}_{sc}$) from the gravity-assist body's velocity ($\vec{v}_{ga}$). Therefore, the flyby time and the $\vec{v}_\infty$ vector yield the full state of the spacecraft and its orbit elements with respect to the central body.

By the patched-conic assumption, the spacecraft's velocity relative the central body ($\vec{v}_{sc}$) is given by the vector sum of the gravity-assist body velocity ($\vec{v}_{ga}$) and the spacecraft's v-infinity ($\vec{v}_\infty$) with respect to the gravity-assist body. This sum is shown both in Eqn. 2 and graphically in Fig. 4.

$$\vec{v}_{sc} = \vec{v}_{ga} + \vec{v}_\infty \tag{2}$$

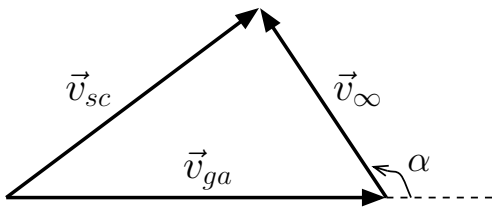

Figure 4. Gravity-Assist Vector Diagram

The angle drawn in Fig. 4 is the *pump* angle (α). Applying the law of cosines to Fig. 4 with our nondimensionalization yields:

$$v_{sc}^2 = 1 + v_\infty^2 + 2v_\infty \cos(\alpha) \tag{3}$$

or, in terms of $\cos(\alpha)$:

$$\cos(\alpha) = \frac{v_{sc}^2 - v_\infty^2 - 1}{2v_\infty} \tag{4}$$

where α is always positive by definition.

Notice that v_{sc} is a function of v_∞ and α. And, by *vis viva*, v_{sc} is directly related to a_{sc} (or v_i for an orbit that is hyperbolic wrt. the central body):

$$v_{sc}^2 = 2 - \frac{1}{a_{sc}} \tag{5}$$

$$v_{sc}^2 = 2 + v_i^2 \tag{6}$$

This then allows us to write a_{sc} as:

$$a_{sc} = 1/\left(1 - v_\infty^2 - 2v_\infty \cos(\alpha)\right) \tag{7}$$

For elliptical and circular orbits, the semi-major axis is directly related to the orbit period (for an ellipse) by Kepler's third law:

$$a_{sc}^3 = T_{sc}^2 \tag{8}$$

Which allows us to write:

$$T_{sc} = \left(1 - v_\infty^2 - 2v_\infty \cos(\alpha)\right)^{-\frac{3}{2}} \tag{9}$$

So if we know the v_∞ magnitude, the pump angle gives us the orbit period (or v_i). Thus, α is a measure of the energy relative to the central body. This relationship is independent of inclination (i_{sc}), i.e. the plane defined by $\vec{v}_{sc}$ and $\vec{v}_\infty$ may be rotated around $\vec{v}_{ga}$ without changing the relations Fig. 4 or Eqn. 3.

The Tisserand Invariant

The theoretical basis for gravity-assists and the method of patched conics was discovered by François Félix Tisserand in 1889[16,18,20] while studying comets that were passing near to Jupiter.[c] Tisserand found a constant[d] from the Jacobi integral that he used to prove the identity of comets whose orbits had been perturbed by a Jupiter flyby. This quantity is now called *Tisserand's Criterion* (C_{Tiss}) and was key to the early development of Gravity-Assist trajectories.[18]

$$C_{Tiss} = \frac{1}{a_{sc}} + 2\cos(i_{sc})\sqrt{a_{sc}(1 - e_{sc}^2)} \tag{10}$$

Rather than derive this constant from the Jacobi integral as in Battin,[16] we shall find it from the $\vec{v}_\infty$. We start with the v_∞ vector in a frame fixed to the gravity-assist body's orbit:[e]

$$\vec{v}_\infty = v_{sc}\sin(\gamma_{sc})\hat{p}_1 + [v_{sc}\cos(\gamma_{sc})\cos(i_{sc}) - 1]\hat{p}_2 + v_{sc}\cos(\gamma_{sc})\sin(i_{sc})\hat{p}_3 \tag{11}$$

[c] Tisserand was studying these comets because his new telescope had a defective mount and couldn't be used to study binary stars as he had originally planned. But, fortunately for future astrodynamicists, the mount was stable enough for observations of Jupiter and Saturn.

[d] Tisserand's criterion is actually only approximately constant in realistic models. But it is close enough to a constant for Tisserand's comets and for preliminary tour designs.

[e] The $\hat{p}_i$-frame is tied to the gravity-assist body's orbit as defined in the Notation section.

Then we square it:

$$v_\infty^2 = v_{sc}^2 + 1 - 2v_{sc}\cos(\gamma_{sc})\cos(i_{sc}) \tag{12}$$

Where $\cos(\gamma_{sc})$ may be found from the conservation of angular momentum to be:

$$\cos(\gamma_{sc}) = \sqrt{a_{sc}(1-e_{sc}^2)} \tag{13}$$

This, with Eqn. 5 yields:

$$v_\infty^2 = 3 - \frac{1}{a_{sc}} - 2\cos(i_{sc})\sqrt{a_{sc}(1-e_{sc}^2)} \tag{14}$$

which then gives an alternate form for Tisserand's Criterion:

$$C_{Tiss} = 3 - v_\infty^2 \tag{15}$$

Therefore, whenever we may assume that v_∞ is constant, we may assume that Tisserand's criterion is also constant.

Equation 14 can be rewritten to provide a very useful relation for e_{sc}:

$$e_{sc}^2 = 1 - \frac{1}{a_{sc}}\left(\frac{3 - \frac{1}{a_{sc}} - v_\infty^2}{2\cos(i_{sc})}\right)^2 \tag{16}$$

This relation holds when the gravity-assist body is in a near circular orbit. It relates v_∞, inclination, period/energy, and eccentricity so that if three are known, the fourth parameter may be solved. This relation is the mathematical basis for tour design using Tisserand Graphs.[10,21,22]

Phase-Free Leveraging

To simplify the analysis, we will assume that the leveraging maneuver occurs at an apse and is tangent to the orbital velocity. The maneuver will be at apoapsis for exterior leveraging and at periapsis for interior leveraging. This assumption limits the effect of the leveraging maneuver to changing the eccentricity without rotating the argument of periapsis. We will also assume that leveraging transfers are in the plane of the gravity-assist body's orbit (i.e. $i_{sc} = 0$).

If we introduce k_{ei} as a constant that is $+1$ for exterior leveraging and -1 for interior leveraging, we can write the radius of the apse where the leveraging maneuver occurs, the *leveraging apse*, r_{la} as:

$$r_{la} = a_{sc}(1 + k_{ei}e_{sc}) \tag{17}$$

Which can be solved for eccentricity:

$$e_{sc} = k_{ei}\left(\frac{r_{la}}{a_{sc}} - 1\right) \tag{18}$$

and then substituting into Eqn. 16 will yield a quadratic in r_{la} and a_{sc} (where C_{Tiss} is a function of v_∞ given by Eqn. 15):

$$4a_{sc}r_{la}^2 - 8a_{sc}^2 r_{la} + a_{sc}^2 C_{Tiss}^2 - 2a_{sc}C_{Tiss} + 1 = 0 \tag{19}$$

This quadratic then yields two roots for r_{la}. One corresponding to $r_{la} > a_{sc}$ (i.e. r_{la} at apoapsis) and the other to $r_{la} < a_{sc}$ (i.e. r_{la} at periapsis). Therefore r_{la} for a given a_{sc} and v_∞ is:

$$r_{la} = a_{sc} + k_{ei}\sqrt{a_{sc}^2 - \frac{1}{4}a_{sc}(3 - v_\infty^2)^2 + \frac{1}{2}(3 - v_\infty^2) - \frac{1}{4a_{sc}}} \tag{20}$$

We now can start with a v'_∞ before the leveraging maneuver and compute r_{la} as a function of a'_{sc} or T'_{sc} or α' of the pre-maneuver orbit. For the post maneuver orbit, r_{la} stays the same and we can use Eqn. 18 and Eqn. 14 to compute v''_∞ as a function of a given a''_{sc}. Alternatively we can use these two equations combined as Eqn. 19 to compute a''_{sc} from v''_∞, but in this case we have to test the two roots for a''_{sc} to find the physically reasonable one. Another approach is to specify the radius of the apse without the maneuver, i.e. the *vacant apse*, r_{va}:

$$r_{va} = 2a_{sc} - r_{la} \tag{21}$$

If r_{la} and r''_{va} are known, we may use Eqn. 21 to solve for a''_{sc} and v''_∞ from Eqn. 14. If $r'_{va} = r''_{va}$ there is no leveraging maneuver and the transfer is ballistic. If either r'_{va} or r''_{va} are equal to one, we have the case of tangent leveraging.

After we have solved for a'_{sc} and a''_{sc}, the ΔV of the leveraging transfer is given by:

$$\Delta V = \left| \sqrt{\frac{2}{r_{la}} - \frac{1}{a'_{sc}}} - \sqrt{\frac{2}{r_{la}} - \frac{1}{a''_{sc}}} \right| \tag{22}$$

We now can calculate phase-free VILTs specified by a parameter before the VILT: $\{v'_\infty$ or $r'_{va}\}$, a parameter after the VILT: $\{v''_\infty$ or $r''_{va}\}$, and a free parameter: $\{r_{la}, a'_{sc}, T'_{sc}$, or $\alpha'\}$. These VILTs are phase-free because we have not yet enforced a constraint that the VILT must encounter the gravity-assist body both before and after the leveraging maneuver. Adding this constraint will allow us to specify a VILT by a combination of spacecraft and gravity-assist body revs for a transfer instead of $\{r_{la}, a'_{sc}, T'_{sc}$, or $\alpha'\}$.

Leveraging Returns

In order to have a VILT return to the gravity-assist body, we must match the flight time of the spacecraft transfer (tof_{sc}) with the time that it takes the gravity-assist body to travel between the encounter locations (tof_{ga}). We must also realize that VILTs can correspond to various numbers of gravity-assist body revolutions, various numbers of spacecraft revolutions, and that the maneuver could occur on any of the spacecraft orbit revs. In addition, the flybys on either end of a VILT can either be *inbound* (i.e. before periapsis) or *outbound* (i.e. after periapsis) as shown in Fig. 5. Both exterior and interior VILTs may be inbound to outbound (IO), inbound to inbound (II), outbound to inbound (OI), or outbound to outbound (OO). For the case where there is no ΔV , IO and OI VILTs become ballistic non-resonant transfers, and II and OO VILTs become ballistic resonant transfers.

For each of the 8 types of VILTs that may be derived from Fig. 5 (i.e. {interior or exterior} and {IO,II,OI, or OO}), there are solutions for various combinations of gravity-assist body revs (N), spacecraft revs (M), and the spacecraft rev number of the maneuver (L). To denote these different cases we will use a modified version of the naming convention of Sims et al.:[8]

$$\{\text{int or ext}\}\text{-}\{\text{IO,II,OI, or OO}\}\ \text{N:M(L)} \tag{23}$$

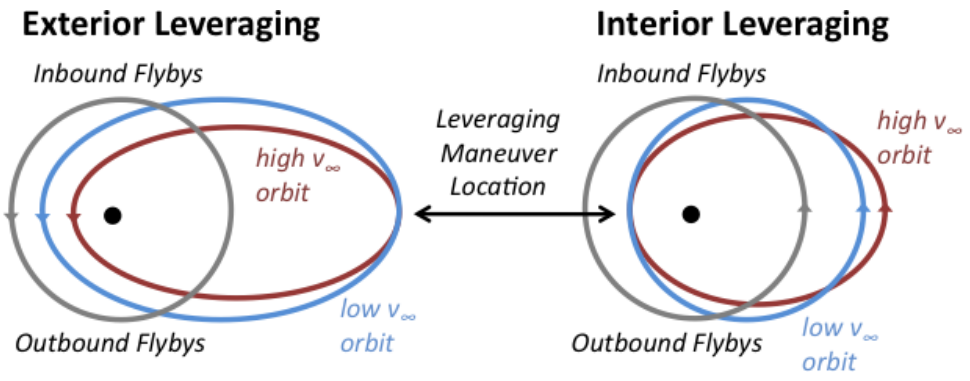

Figure 5. Inbound and Outbound Flybys

Examples of this naming convention would be: int-OI 2:3(1), ext-OO 1:1(0), int-IO 0:0(0), ext-II 12:11(7), etc.

We can enforce the return constraint by matching the flight time between flyby locations of the spacecraft (tof_{sc}) to that of the gravity-assist body (tof_{ga}). To find tof_{sc} we start by solving for the eccentric anomaly:[f]

$$E_{sc} = k_{io} \cos^{-1}\left(\frac{a_{sc} - 1}{e_{sc} a_{sc}}\right) \tag{24}$$

where k_{io} is $+1$ for an outbound encounter and -1 for an inbound encounter. From E_{sc} we can now get the time from periapsis of the encounter in the spacecraft's orbit (where $T_{sc} = (a_{sc})^{3/2}$):

$$\tau_{sc} = \frac{T_{sc}}{2\pi}\left(E_{sc} - e_{sc}\sin(E_{sc})\right) \tag{25}$$

By thoughtful inspection of Fig. 5 we can derive the following relations for tof_{sc} for the 8 kinds of VILTs:[g]

exterior	IO,II, or OO	$tof_{sc} = (\tau''_{sc} - \tau'_{sc}) + T'_{sc}(L + 1/2) + T''_{sc}(M - L - 1/2)$	(26)
exterior	OI	$tof_{sc} = (\tau''_{sc} - \tau'_{sc}) + T'_{sc}(L + 1/2) + T''_{sc}(M - L + 1/2)$	(27)
interior	IO,II, or OO	$tof_{sc} = (\tau''_{sc} - \tau'_{sc}) + T'_{sc}L + T''_{sc}(M - L)$	(28)
interior	OI	$tof_{sc} = (\tau''_{sc} - \tau'_{sc}) + T'_{sc}L + T''_{sc}(M - L + 1)$	(29)

By using k_{ei} and M_a we can simplify the four equations above into one equation:

$$tof_{sc} = \tau''_{sc} - \tau'_{sc} + T'_{sc}\left(L + \frac{1 + k_{ei}}{4}\right) + T''_{sc}\left(M_a - L - \frac{1 + k_{ei}}{4}\right) \tag{30}$$

where M_a is the number of spacecraft revs counted by apoapsis crossings and is related to M as follows:

$$M_a = \begin{cases} M & \text{if IO,II, or OO} \\ M + 1 & \text{if OI} \end{cases} \tag{31}$$

[f]For the one hyperbolic VILT, an $M = 0$ IO transfer, the analogous equations for hyperbolic anomaly would have to be used instead of Eqn. 24 and Eqn. 25.

[g]Remember that τ_{sc} has the same sign as k_{io}.

Equation 30 accounts for the time of flight of the spacecraft. The next part is to account for the time of flight of the gravity-assist body. Since we have assumed the gravity-assist body to be in a circular orbit we can find its flight time from the angle between the two encounters. The true anomaly of each encounter is given by:

$$f_{sc} = k_{io} \cos^{-1}\left(\frac{1}{e_{sc}}(a_{sc}(1-{e_{sc}}^2)-1)\right) \tag{32}$$

Then the flight time of the gravity assist body is:

$$tof_{ga} = N_a + \frac{1}{2\pi}(f''_{sc} - f'_{sc}) \tag{33}$$

where, like M_a, N_a is introduced to cover the OI case. Here N_a is the number of times that the gravity-assist body crosses the line between the central body and spacecraft apoapsis. N_a is given by:

$$N_a = \begin{cases} N & \text{if IO,II, or OO} \\ N+1 & \text{if OI} \end{cases} \tag{34}$$

Since we need to use Kepler's equation to get τ'_{sc} and τ''_{sc} in Eqn. 30 we cannot start from the constraint $tof_{sc} = tof_{ga}$ and work backwards to find the VILT. Rather we have to iteratively guess phase-free VILTs until this constraint is met. We do this by guessing one of the free parameters of the phase free problem, $\{r_{la}, a'_{sc}, T'_{sc}$, or $\alpha'\}$, and iterating to find the value where:

$$tof_{sc} = tof_{ga} \tag{35}$$

Each of the solutions to Eqn. 35 gives a VILT specified by the naming convention in Eqn. 23.

Tisserand Graph

A *Tisserand graph*[10–12,21,22] may be used to better understand how VILTs and flybys help us access new orbits around the central body. It can also help us visualize families of VILTs specified by Eqn. 23. Figure 6 is an example of such a Tisserand graph.

Figure 6 is a Tisserand graph showing apoapsis radius (r_a) versus periapsis radius (r_p). Each point on the graph represents an orbit around the central body. Since Tisserand's criterion remains constant through flybys, we may plot contours with constant values of Tisserand's criterion or v_∞ ($C_{Tiss} = 3 - v_\infty^2$) to represent how flybys can change the orbit with respect to the central body. We may also plot other lines to show orbits associated with particular VILTs. The diagonal line (connecting points C and F) is an example of this, showing orbits after a leveraging maneuver that reencounter the gravity-assist body. This line is for ext-II 4:3(0) VILTs starting from v'_∞. Each point on the line is associated with a different v''_∞ for the orbit after the maneuver.

In Fig. 6, we can start from the orbit at point 'A' and use a flyby to move along the v'_∞ contour to reach point 'B'. For exterior leveraging, the apoapsis radius (i.e. $r_{la} = r_a$) doesn't change during the maneuver. This means that the VILT follows a line of constant apoapsis on this Tisserand graph from point 'B' to point 'C'. The orbit at point 'C' then re-encounters the gravity-assist body and additional flybys may be used to move along the v''_∞ contour. Since point 'C' is closer to the $r_p = 1$ line, we have made our orbit less eccentric with the VILT, and we have lowered v_∞.

We may chose other points along the v'_∞ contour in Fig. 6 to start our VILT. If we do more bending with the initial flyby we may move from 'A' to 'D'. From point 'D' our VILT will raise

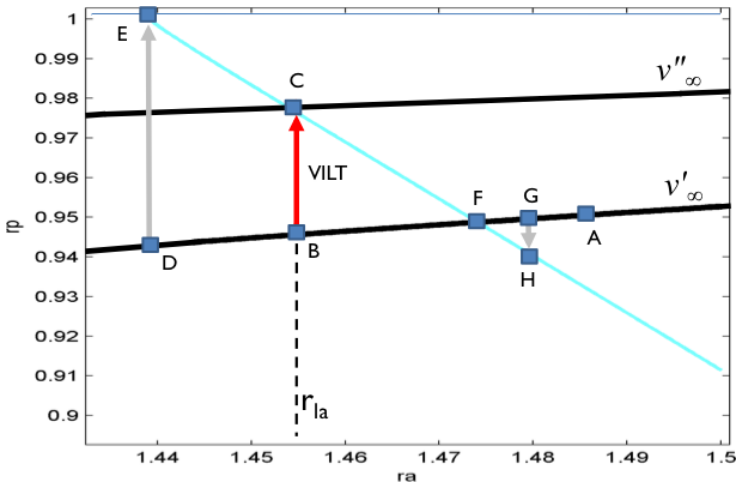

Figure 6. Example of External VILT

periapsis to 1, and we have the tangent leveraging case. Alternatively, we can do less bending and move from 'A' to 'F'. At point 'F', no leveraging maneuver is needed to re-encounter the gravity-assist body and we have the ballistic transfer case. What if we cannot do enough bending with our flyby to even reach 'F', and we reach our flyby altitude constraint at point 'G'? From 'G' we can still reach this VILT family by increasing v_∞ and moving to point 'H'. Although our final goal may be to reduce v_∞, we may be willing to expend some ΔV to increase v_∞ if the VILT has an attractive flight time. Such (non-intuitive) low-bending VILTs are very useful when designing low flight-time tours with low-mass moons.

EXAMPLE TOUR

We will now use the techniques that we have developed to design an example *leveraging tour* (i.e. a tour with VILTs) that starts from Saturn arrival condition similar to that of the Titan Saturn System Mission (TSSM) study[2,23] and reaches Enceladus orbit. This tour is intended to be an example of how leveraging techniques can improve upon the Enceladus orbit insertion from a direct Titan to Enceladus transfer, and is not intended to represent an optimal solution to the problem. We do not wish to tie the solution to a specific epoch and will not consider the phasing of the transfer orbits between the moons. Including these transfer orbits would add a small amount of additional flight time to our estimates (on the order of a few revs of the moons involved). However, the additional ΔV from these transfers will be negligible.

Table 2. Initial Saturn Orbit

TSSM SOI	746 m/s	Initial r_p	1.2 R_S
Pre-SOI Mass	5814 kg	Initial r_a	200 R_S
Flight Time to SOI	9 yrs	Initial T_{sc}	180 days

Table 2 gives the Saturn arrival conditions for the TSSM study.[2,23] We use these parameters as a starting point for designing our trajectory to Enceladus and for comparison with other methods. On arrival at Saturn, the TSSM mission uses a 746 m/s Saturn Orbit Insertion (SOI) maneuver to

enter an initial 1.2 Saturn radii by 200 Saturn radii orbit. From this orbit, we use a 564 m/s Periapsis Raise Maneuver (PRM)[h] to raise the periapsis to Titan's orbit and achieve a v_∞ of 1.46 km/s. Table 3 shows the three flybys and one leveraging maneuver used to transition from the post-PRM orbit to a Titan-Rhea Hohmann transfer. Figure 7 shows these flybys and the leveraging on a Tisserand graph.

Table 3. Titan Transfers

Flyby	tof [d]	Altitude [km]	Transfer Type N:M(L)	v'_∞ [km/s]	v''_∞ [km/s]	ΔV [m/s]
Titan-1	31.5	2290	ext-OO 2:1(0)	1.46	1.27	27.4
Titan-2	21.3	3010	OI 1:1	1.27	1.27	0.0
Titan-3	—	15220	*transfer to Rhea*			

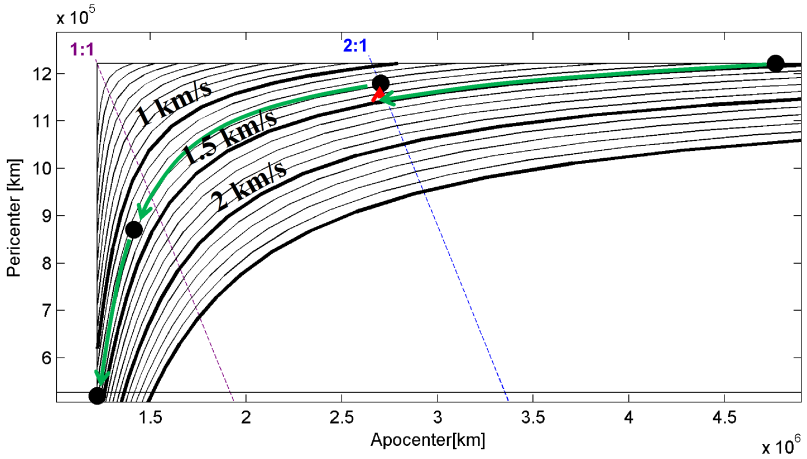

Figure 7. Titan Leveraging

Table 4 and Fig. 8 show the 14 Rhea flybys and 8 leveraging maneuvers needed to get from the Titan-Rhea Hohmann to the Rhea-Dione Hohmann. This sequence of VILTs and ballistic transfers requires 10 months and 251 m/s. The minimum flyby altitude allowed for Rhea (as well as Dione and Tethys) is 50 km. Some of these encounters are very close in time from an operational perspective, and a future mission's ground system may not be able to handle flybys closer than 9 days. However, we chose to design a tour without presupposing any particular constraints from the ground system with the assumption that such a tour could be modified by adding transfers with multiple spacecraft revs if needed.

In Table 4, flybys Rhea-3 and Rhea-9 are particularly interesting in that they increase v_∞. If the goal of this sequence of flybys is to lower v_∞ from the initial 1.75 km/s to near the Rhea-Dione Hohmann's 0.73 km/s, why is ΔV used to increase v_∞? The answer can be found in the earlier discussion of points 'G' and 'H' on Fig. 6 where v_∞ was increased in order the reach a desired VILT with low-bending. The flybys before the VILT were already at or near the 50 km limit and could not provide enough bending to reach the ballistic transfer. By increasing v_∞, the 50 km flyby provided enough bending to reach the desired ext-IO 11:6(2) VILT.

[h]In fact, PRM is also a leveraging maneuver.

The Dione transfers are shown in Table 5 and Fig. 9, taking 3.6 months and 90 m/s. The Tethys transfers in Table 6 and Fig. 10 then go from Dione to Enceladus in 4.4 months with 28 m/s. Finally, in Table 7 and Fig. 11, 4.8 months and 96 m/s of Enceladus leveraging is used to reduce the Enceladus v_∞ from 800 m/s to 300 m/s. Due to Enceladus' small mass, we allowed the minimum flyby altitude during this segment to decrease to 40 km initially and then to 25 km at the end. Although we believe that such low flybys should be possible at Enceladus, a future project may find it preferable to do orbit insertion from a higher v_∞ rather than develop ground and flight systems capable of such low flybys.

Table 4. Rhea Transfers

Flyby	tof [d]	Altitude [km]	Transfer Type N:M(L)	v'_∞ [km/s]	v''_∞ [km/s]	ΔV [m/s]
Rhea-1	9.0	140	OO 2:1	1.75	1.75	0.0
Rhea-2	17.4	4910	OI 2:1	1.75	1.75	0.0
Rhea-3	50.4	50	ext-IO 11:6(2)	1.75	1.76	1.4
Rhea-4	38.7	470	OI 7:4	1.76	1.76	0.0
Rhea-5	37.1	50	ext-IO 8:5(4)	1.76	1.77	2.0
Rhea-6	13.2	60	ext-OO 3:2(1)	1.77	1.21	99.1
Rhea-7	31.5	50	ext-OO 7:5(4)	1.21	1.02	29.7
Rhea-8	17.9	510	ext-OO 4:3(0)	1.02	0.88	24.1
Rhea-9	31.4	50	ext-OI 6:5(0)	0.88	0.90	5.0
Rhea-10	6.5	60	ext-IO 1:1(0)	0.90	0.99	35.7
Rhea-11	6.2	240	OI 1:1	0.99	0.99	0.0
Rhea-12	26.9	80	int-II 6:7(5)	0.99	0.75	53.6
Rhea-13	18.1	200	II 4:5	0.75	0.75	0.0
Rhea-14	—	6990	*transfer to Dione*			

Table 5. Dione Transfers

Flyby	tof [d]	Altitude [km]	Transfer Type N:M(L)	v'_∞ [km/s]	v''_∞ [km/s]	ΔV [m/s]
Dione-1	13.6	100	ext-OO 5:4(3)	0.90	0.82	12.0
Dione-2	19.3	160	ext-OI 6:5(0)	0.82	0.70	21.5
Dione-3	24.6	110	II 9:8	0.70	0.70	0.0
Dione-4	3.9	60	ext-IO 1:1(0)	0.70	0.77	30.4
Dione-5	3.8	220	OI 1:1	0.77	0.77	0.0
Dione-6	26.5	50	int-IO 9:10(9)	0.77	0.70	17.9
Dione-7	16.7	180	int-OI 6:7(6)	0.70	0.65	8.4
Dione-8	—	970	*transfer to Tethys*			

Table 8 shows the combined ΔV of these transfers along with the TSSM SOI ΔV and a PRM ΔV calculated from the TSSM initial orbit. The Enceladus orbit insertion is calculated with a 10% estimate of gravity losses. Tour statistical ΔV is estimated at 5 m/s per flyby. The table also

Table 6. Tethys Transfers

Flyby	tof [d]	Altitude [km]	Transfer Type N:M(L)	v'_∞ [km/s]	v''_∞ [km/s]	ΔV [m/s]
Tethys-1	13.4	790	OI 6:5	0.77	0.77	0.0
Tethys-2	13.3	110	ext-II 7:6(0)	0.77	0.70	12.1
Tethys-3	17.0	60	II 9:8	0.70	0.70	0.0
Tethys-4	26.4	50	II 14:13	0.70	0.70	0.0
Tethys-5	2.7	50	IO 1:1	0.70	0.70	0.0
Tethys-6	1.9	510	OO 1:1	0.70	0.70	0.0
Tethys-7	2.6	480	OI 1:1	0.70	0.70	0.0
Tethys-8	25.8	50	int-IO 13:14(2)	0.70	0.67	10.3
Tethys-9	17.3	150	OI 9:10	0.67	0.67	0.0
Tethys-10	13.2	130	int-II 7:8(7)	0.67	0.63	5.3
Tethys-11	—	270	*transfer to Enceladus*			

Table 7. EnceladusTransfers

Flyby	tof [d]	Altitude [km]	Transfer Type N:M(L)	v'_∞ [km/s]	v''_∞ [km/s]	ΔV [m/s]
Enceladus-1	9.6	40	OO 7:6	0.80	0.80	0.0
Enceladus-2	20.6	30	ext-OO 15:13(3)	0.80	0.82	3.2
Enceladus-3	12.3	40	ext-OI 8:7(5)	0.82	0.75	13.1
Enceladus-4	23.5	40	ext-IO 17:15(8)	0.75	0.60	25.5
Enceladus-5	12.3	40	OO 9:8	0.60	0.60	0.0
Enceladus-6	13.7	40	ext-OO 10:9(8)	0.60	0.50	16.6
Enceladus-7	15.1	30	ext-OO 11:10(0)	0.50	0.52	2.0
Enceladus-8	17.7	30	ext-OO 13:12(11)	0.52	0.37	25.6
Enceladus-9	19.1	25	ext-OO 14:13(1)	0.37	0.30	10.4

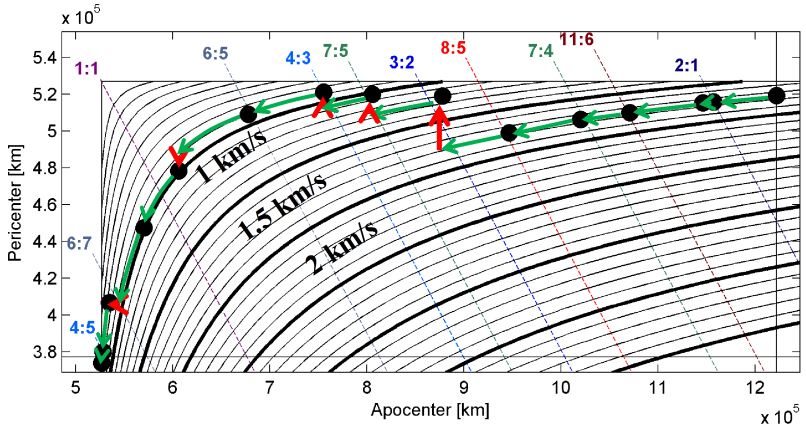

Figure 8. Rhea Leveraging

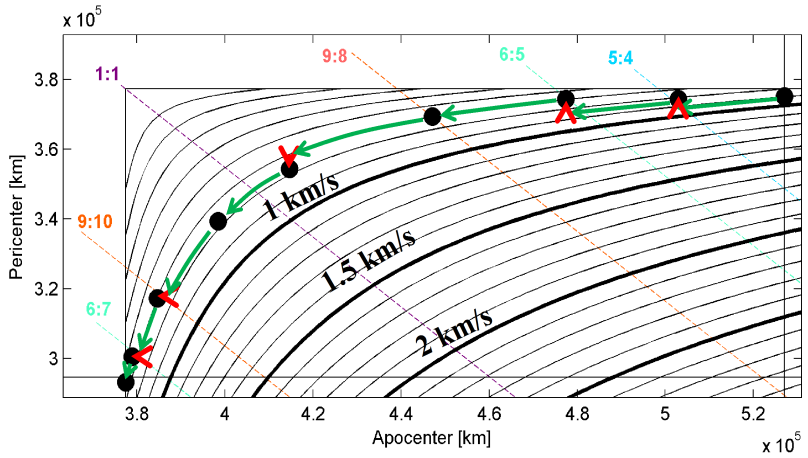

Figure 9. Dione Leveraging

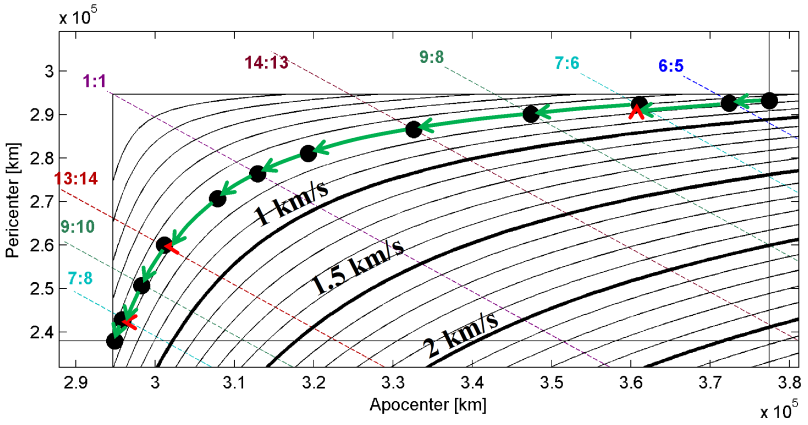

Figure 10. Tethys Leveraging

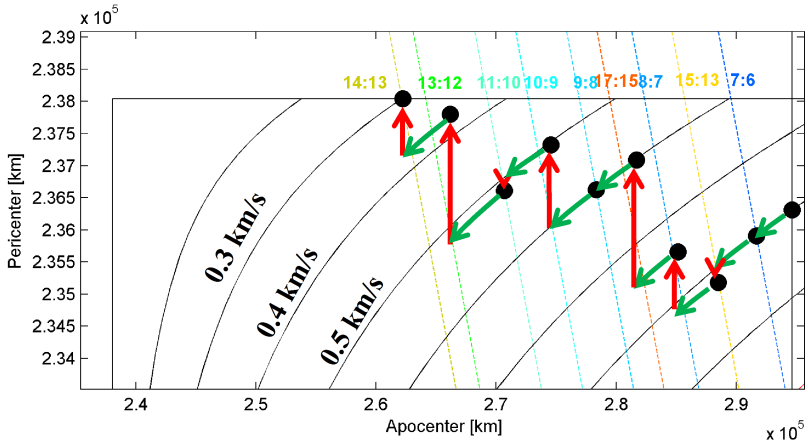

Figure 11. Enceladus Leveraging

shows ΔV totals for two alternate strategies[i] for reaching Enceladus: inserting directly from a Titan-Enceladus Hohmann, and inserting directly from the initial TSSM orbit. The ΔV for each strategy is then used with the TSSM bi-prop Isp of 323 sec. to calculate a mass inserted into Enceladus orbit assuming the TSSM Saturn arrival mass of 5814 kg. From Enceladus orbit, the spacecraft may use additional ΔV for orbit maintenance, orbit changes, and/or for landing on Enceladus, but this ΔV is not accounted for in this analysis. Finally, for each strategy, an approximate flight time is estimated that does not account for phasing orbits that may be needed to transfer between the moons.

This example leveraging tour places into Enceladus orbit 250% of the mass into orbit of the Titan-Enceladus Hohmann and 350% of the mass of a direct insertion after SOI. It does this with an increase of flight time to 2.5 years. With the 9 year flight time to Saturn of the TSSM trajectory, that would leave a mission with up to 2.5 years at Enceladus before the 14 year qualification lifetime of the Radioisotope Power System (RPS) would be reached. This longer flight time also allows exciting science from 14 Rhea flybys, 8 Dione flybys, and 11 Tethys flybys, all of which are at much lower encounter speeds than the handful of Cassini flybys of these bodies. Furthermore, this is just one example tour and other tours exist with different combinations of flight time and ΔV.

Table 8. Delta-V Comparison

	Leveraging Tour	Titan-Encel.	SOI-Encel.
SOI [m/s]	746	746	746
PRM [m/s]	564	546	159
Titan Leveraging [m/s]	27	—	—
Rhea Leveraging [m/s]	251	—	—
Dione Leveraging [m/s]	90	—	—
Tethys Leveraging [m/s]	28	—	—
Encel. Leveraging [m/s]	96	—	—
Tour Statistical ΔV Est. [m/s]	225	20	—
Encel. Orbit Insertion [m/s]	242	3,933	5,380
Total ΔV [m/s]	2,269	5,245	6,285
Encel. On-Orbit Mass [kg]	2,839	1,109	798
TOF from SOI [yr]	$\sim$2.5	$\sim$0.7	$\sim$0.5

CONCLUSION & FUTURE WORK

A Leveraging tour with Titan, Rhea, Dione, and Tethys can reach Enceladus orbit with less than half of the ΔV of a direct Titan-Enceladus transfer. Starting from the TSSM Saturn arrival conditions, with a chemical bi-prop system the Leveraging tour places into Enceladus orbit 2.5$\times$ the mass of the Titan-Enceladus transfer. This may be done with flight times around 2.5 years from SOI. Moreover, this leveraging tour provides many low-speed and high science value flybys of Rhea, Dione, and Tethys.

[i]The flight times for all of the strategies include 0.5 year for the initial orbit. The Titan-Enceladus strategy includes an estimate of 0.2 year for Titan flybys, and the Leveraging Tour includes 2 years for the flybys described in Tables 3-7.

To build this leveraging tour we have developed a new method to construct non-tangent V-Infinity Leveraging Transfers (VILTs). These VILTs provide additional flexibility when constructing tours using low mass moons and may be used to access low flight time transfers for which the moon would otherwise provide insufficient bending to reach.

In the future, we plan to further develop the graphical design methods using the Tisserand graphs and to develop strategies for designing Leveraging tours to traverse these Tisserand graphs. We also plan to integrate and optimize these leveraging tours in a full force model.

ACKNOWLEDGMENT

Research described in this paper was carried out at the Jet Propulsion Laboratory, California Institute of Technology, under contract with the National Aeronautics and Space Administration.

NOMENCLATURE

Variables

α	pump angle	$\hat{p}_3$	$= \frac{\hat{r}_{enc} \times \hat{v}_{ga}}{\cos(\gamma_{ga})}$
γ	flight path angle	r	distance from center of body
δ	flyby bending angle	r_a	apoapsis radius wrt cb
μ	gravitational parameter	r_{enc}	radius of flyby encounter location wrt cb
τ	time wrt periapsis	r_{la}	radius of leveraging apse wrt cb
a	semi-major axis	r_p	periapsis radius wrt cb
C_{Tiss}	Tisserand invariant	r_{pfb}	periapsis radius wrt ga-body
E	eccentric anomaly	R_S	Saturn radius, 60330 km.
e	eccentricity	r_{va}	radius of vacant apse wrt cb
f	true anomaly	T	orbit period
i	inclination wrt ga-body orbit	T_c	circular orbit period at r_{enc}
L	rev number of maneuver	tof	time of flight between encounters
M	number of s/c orbits	v	velocity
M_a	number of s/c apoapses	v_∞	hyperbolic excess velocity wrt ga-body
N	number of ga-body orbits	v_a	velocity at apoapsis wrt cb
N_a	N counted by s/c apoapsis	v_c	circular velocity wrt cb at r_{enc}
$\hat{p}_1$	$= \hat{r}_{enc}$	v_i	hyperbolic excess velocity wrt cb
$\hat{p}_2$	$= \hat{p}_3 \times \hat{p}_1$	v_p	velocity at periapsis wrt cb

Subscripts / Superscripts

x_{cb}	'x' pertains to central body
x_{fb}	'x' pertains to patched-conic spacecraft orbit relative to gravity assist body at encounter
x_{ga}	'x' pertains to gravity-assist body orbit relative to central body at encounter
x_{sc}	'x' pertains to patched-conic spacecraft orbit relative to central body at encounter
x'	'x' is quantity before leveraging maneuver
x''	'x' is quantity after leveraging maneuver

Vectors

$\vec{x}$ 'x' is a vector $\hat{x}$ 'x' is a unit vector x 'x' is a vector magnitude

REFERENCES

[1] "Enceladus Flagship Mission concept Study," NASA Goddard Space Flight Center, August 29, 2007. *See also: http://opfm.jpl.nasa.gov/library/*

[2] "Titan Saturn System Mission Final Report on the NASA Contribution to a Joint Mission with ESA," Jet Propulsion Laboratory, January 30, 2009. *See also: http://opfm.jpl.nasa.gov/library/*

[3] R.P. Russell and M.P. Lara, "On the Design of an Enceladus Science Orbit," *Acta Astronautica*, V. 65, No. 1-2, p. 27-39.

[4] T.R. Spilker, R.C. Moeller, C.S. Borden, W.D. Smythe, R.E. Lock, J.O. Elliott, J.A. Wertz, N.J. Strange, "Analysis of Architectures for the Scientific Exploration of Enceladus, IEEEAC Paper 1644, 2009 IEEE Aerospace conference, Mar. 2009.

[5] S.N. Williams, "Automated Design of Multiple Encounter Gravity-Assist Trajectories," M.S. Thesis, School of Aeronautics and Astronautics, Purdue Univ., West Lafayette, IN, Aug. 1990.

[6] C. Uphoff, P. H. Roberts, and L. D. Friedman, "Orbit Design Concepts for Jupiter Orbiter Missions," AIAA Mechanics and Control Conference, AIAA Paper 74-781, Anaheim, California, Aug. 1974.

[7] J.A. Sims and J.M. Longuski, "Analysis of V_∞ Leveraging for Interplanetary Missions," AIAA Paper 94-3769, Aug. 1994.

[8] J.A. Sims, J.M. Longuski, and A. Staugler, "V-innity Leveraging for Interplanetary Missions: Multiple-Revolution Orbit Techniques," *Journal of Guidance, Control and Dynamics*, Vol. 20, No. 3, 1997, pp. 409415.

[9] G. Hollenbeck, "New Flight Techniques for Outer Planet Missions," AAS Paper 75-087, AIAA/AAS Astrodynamics Specialist Conference, Nassau, Bahamas, Jul. 1975.

[10] N.J. Strange and J.A. Sims, "Methods for the Design of V-Infinity Leveraging Maneuvers," AAS Paper 01-473, AAS/AIAA Astrodynamics Conference, Québec, Québec, July/Aug. 2001.

[11] S. Campagnola and R.P. Russell, "The Endgame Problem Part A: V-Infinity Leveraging Technique and The leveraging Graph," AAS Paper 09-224, AAS/AIAA Space Flight Mechanics Meeting, Savannah, GA, Feb. 2009.

[12] S. Campagnola and R.P. Russell, "The Endgame Problem Part B: The Multi-Body Technique and the T-P Graph," AAS Paper 09-227, AAS/AIAA Space Flight Mechanics Meeting, Savannah, GA, Feb. 2009.

[13] A.T. Brinckerhoff and R.P. Russell, "Pathfinding and V-Infinity Leveraging for Planetary Moon Tour Missions," AAS Paper 09-222, AAS/AIAA Space Flight Mechanics Meeting, Savannah, GA, Feb. 2009.

[14] R.P. Russell and C.A. Ocampo, "Geometric Analysis of Free-Return Trajectories Following a Gravity-Assisted Flyby," *Journal of Spacecraft and Rockets*, Vol. 42, No. 1, 2005, pp. 138-151.

[15] M. Vasile and S. Campagnola, "Design of Low-Thrust Multi-Gravity Assist Trajectories to Europa," *Journal of the British Interplanetary Society*, Vol. 62, No. 1, Jan. 2009, pp. 15-31.

[16] R.H. Battin, *An Introduction to the Mathematics and Methods of Astrodynamics, Revised Edition*, AIAA Press, Reston, Va., 1999.

[17] R.A. Brouke, "The Celestial Mechanics of Gravity Assist," AIAA/AAS Astrodynamics Conference, AIAA Paper 88-4220, Minneapolis, Minnesota, Aug. 1988.

[18] R.A. Brouke, "On the History of the Slingshot Effect and Cometary Orbits," AAS/Astrodynamics Specialist Conference, AAS Paper 01-435, Québec, Québec, Jul.-Aug. 2001.

[19] R.J. Cesarone, "A Gravity Assist Primer," *AIAA Student Journal*, Vol. 16, Spring 1989, pp. 16-22.

[20] F.F. Tisserand, *Traite de Mechanique Celeste*, Vol. 4. Gauthier-Villars et ls, 1896.

[21] N.J. Strange and J.M. Longuski, "Graphical Method for Gravity-Assist Trajectory Design," *Journal of Spacecraft and Rockets*, Vol. 39, No. 1, Jan. 2001, pp. 9-16.

[22] A.V. Labunsky, O.V. Papkov, K.G. Sukhanov, *Multiple Gravity Assist Interplanetary Trajectories*, Gordon and Breach Science Publishers, Newark, NJ, 1998, pp. 3354.

[23] N.J. Strange, T.R. Spilker, D.F. Landau, T. Lam, D.T. Lyons, and J.J. Guzman, "Mission Design for the Titan Saturn System Mission Concept," AAA Paper 09-356, AAS/AIAA Astrodynamics Conference, Pittsburgh, PA, Aug. 2009.